

Highly Elastic Micropatterned Hydrogel for Engineering Functional Cardiac Tissue

Nasim Annabi, Kelly Tsang, Suzanne M. Mithieux, Mehdi Nikkhah, Afshin Ameri, Ali Khademhosseini,* and Anthony S. Weiss*

Heart failure is a major international health issue. Myocardial mass loss and lack of contractility are precursors to heart failure. Surgical demand for effective myocardial repair is tempered by a paucity of appropriate biological materials. These materials should conveniently replicate natural human tissue components, convey persistent elasticity, promote cell attachment, growth and conformability to direct cell orientation and functional performance. Here, microfabrication techniques are applied to recombinant human tropoelastin, the resilience-imparting protein found in all elastic human tissues, to generate photocrosslinked biological materials containing well-defined micropatterns. These highly elastic substrates are then used to engineer biomimetic cardiac tissue constructs. The micropatterned hydrogels, produced through photocrosslinking of methacrylated tropoelastin (MeTro), promote the attachment, spreading, alignment, function, and intercellular communication of cardiomyocytes by providing an elastic mechanical support that mimics their dynamic mechanical properties *in vivo*. The fabricated MeTro hydrogels also support the synchronous beating of cardiomyocytes in response to electrical field stimulation. These novel engineered micropatterned elastic gels are designed to be amenable to 3D modular assembly and establish a versatile, adaptable foundation for the modeling and regeneration of functional cardiac tissue with potential for application to other elastic tissues.

1. Introduction

Treatment of cardiac injury is severely limited by the inability of myocardium to regenerate after injury, insufficient allograft tissue for transplantation, and the marked ineffectiveness of current therapies to induce adequate myocardium regeneration.^[1] Therefore, there is major interest in developing new strategies to generate implantable functional cardiac tissue constructs. A promising approach for myocardial repair would be to combine biocompatible scaffolds with cells followed by implantation of engineered tissue constructs within the injured heart.^[2–4] However, there is a paucity of materials that would be suitable for this task. To achieve this goal, it is necessary for the engineered tissues to mimic the structural and functional properties of native myocardium.^[2,5,6] An ideal scaffold for cardiac tissue engineering needs to convey a blend of relevant mechanical and biological properties to facilitate cardiomyocyte (CM) attachment and growth,

Dr. N. Annabi, K. Tsang, Dr. M. Nikkhah,
A. Ameri, Prof. A. Khademhosseini
Center for Biomedical Engineering
Department of Medicine
Brigham and Women's Hospital
Harvard Medical School
Boston, MA 02139, USA
Harvard-MIT Division of Health Sciences and Technology
Massachusetts Institute of Technology
Cambridge, MA 02139 USA
E-mail: alik@rics.bwh.harvard.edu
Dr. N. Annabi, Prof. A. Khademhosseini
Wyss Institute for Biologically Inspired Engineering
Harvard University
Boston, MA, 02115, USA
K. Tsang
Department of Materials Engineering
Monash University
Melbourne, Victoria, Australia

Dr. S. M. Mithieux, Prof. A. S. Weiss
School of Molecular Bioscience
University of Sydney
Sydney, 2006, Australia
E-mail: tony.weiss@sydney.edu.au
Prof. A. S. Weiss
Charles Perkins Centre
University of Sydney
Sydney, 2006, Australia
Prof. A. S. Weiss
Bosch Institute
University of Sydney
Sydney, 2006, Australia



DOI: 10.1002/adfm.201300570

promote cellular alignment and elongation, and provide the flexibility and capacity for sustained cycles of expansion and contraction.

Major problems with current cardiac tissue engineered scaffolds encompass the risks of toxicity, immunogenicity, lack of compatible degradation paths, and inappropriate mechanical performance.^[3–5] Common tissue engineering polyesters such as polylactic acid (PLA), and polyglycolic acid (PGA) degrade to generate acidic byproducts, display irregular degradation kinetics that can lead to the sudden deterioration of the construct's mechanical properties^[7] and are more rigid than heart tissue.^[8] Although elastomeric polymers such as polyurethane are more elastic, their diisocyanate degradation products are toxic.^[5] Microfabricated elastomer poly(glycerol sebacate) (PGS) scaffolds with structural and mechanical properties similar to that of myocardium have been produced^[9] but PGS-based scaffolds degrade rapidly by surface hydrolysis with a mass loss of 70% and a linear decrease in mechanical strength of 8% per week over 35 days of implantation.^[10]

Matrigel and natural collagen-based hydrogels provide potentially favorable microenvironments for cardiac tissue formation but they present a range of limitations that include poor mechanical stability and suboptimal durability.^[11,12] The clinical use of animal-derived extracellular matrix (ECM) proteins is often restricted due to immunogenic concerns^[13,14] and the risk of cross-species infection. On the other hand, stiffer scaffolds such as non-woven PGA tend to limit the beating amplitude of CMs.^[15,16] Elastic substrates promote myocyte growth and function as they better mimic the dynamic mechanical properties of myocytes in vivo compared to rigid substrates.^[17] To address these multiple challenges, we coupled an advanced elastic biomaterial based on a recombinant human tropoelastin with microfabrication techniques to develop highly elastic, biologically compatible, micropatterned substrates for myocardium regeneration.

Tropoelastin is the dominant physiological component of elastin, where upon crosslinking it conveys elasticity, extraordinary stability and persistence, and cell-interactive biological activity. It is logical to adapt this large biological polymer to bioengineering applications but the generation of microfabricated tropoelastin-based hydrogels containing well-defined micrometer-sized patterns has been limited due to the traditional crosslinking routes, which result in the formation of amorphous unstructured hydrogels with low mechanical stability.^[18–20] Recently, we have shown that photocrosslinked tropoelastin hydrogels are formed in less than a minute by UV crosslinking of methacrylated tropoelastin (MeTro).^[21] The fabricated hydrogels exhibit remarkable mechanical characteristics such as high resilience upon stretching with extensibility up to 400% and reversible deformation with low energy loss. In addition, we found that the mechanical properties of fabricated MeTro gels can be finely tuned to select desirable stiffness for a specific application. For example, their elastic moduli are in the range of 2.8 ± 0.6 to 14.8 ± 1.9 kPa and ultimate strengths range from 12.5 ± 2.2 kPa to 39.3 ± 2.5 kPa depending on the methacrylation degree and concentration of MeTro.^[21] These properties make MeTro gel a promising hydrogel for engineering soft, elastic tissues such as cardiac and vascular tissues.

In this study, we combine MeTro hydrogels with microfabrication techniques with the aim of developing highly elastic micro-engineered hydrogels for cardiac tissue engineering applications. MeTro gels are formed from human tropoelastin which is a water-soluble protein, containing 35 lysine residues per molecule, that confers integrin-based cell-binding sites.^[22] We show that the use of this human protein in the formulation of MeTro gel promotes CM adhesion and growth. In addition, we integrated micropatterns on the surfaces of these hydrogels for CM alignment to engineer tissue constructs mimicking those of the native myocardium. Furthermore, we found that the system is compatible with electrical stimulation, which we used to modulate the contractile properties of CMs seeded on these MeTro hydrogels.

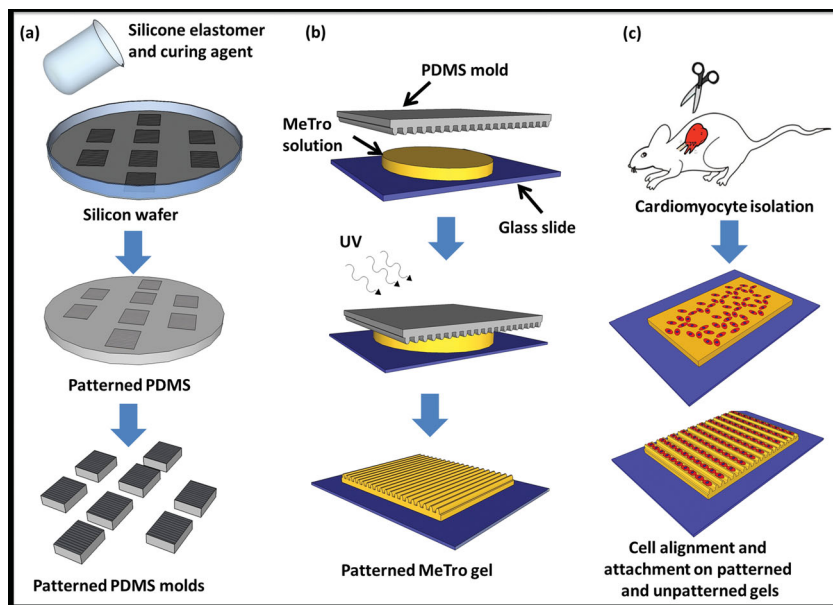
2. Results and Discussion

In this study, we fabricated a new class of highly elastic micropatterned hydrogels from MeTro for cardiac tissue regeneration where elasticity plays an important role in tissue functionality.^[23] Microfabrication technologies were used to generate high-resolution microchannels on the surfaces of these hydrogels to guide cellular orientation and elongation and further improve the functionality of engineered constructs (**Scheme 1**).

2.1. CM Attachment and Spreading on MeTro Hydrogels

We have previously demonstrated that MeTro gels can accommodate embedded and surface cells.^[21] Here, we sought to demonstrate the formation, alignment, and maintenance of CM phenotype on the microfabricated MeTro gels. Cardiac tissue is known to rely on matrix elasticity to maintain cell viability, organization, and tissue function.^[23] Neonatal rat CM growth was evaluated on MeTro hydrogels and compared to methacrylated gelatin (GelMA) gels. GelMA is an attractive hydrogel for creating micropatterned tissue constructs.^[24,25] CM attachment, proliferation, and spreading on MeTro and GelMA hydrogels were assessed after 8, 24, 72 and 192 h of culture using nuclei and F-actin staining (**Figure 1a–h**). After 8 h, 2.5 times more cells had adhered to the surface of MeTro (564 ± 133 cells mm^{-2}) than on GelMA (225 ± 47 cells mm^{-2}) gels (**Figure 1i**). Although both hydrogels supported cell proliferation, as demonstrated by an increasing number of nuclei over the 8-day culture period, proliferation rates were higher ($p < 0.001$) on MeTro.

The spreading of CMs on MeTro gels began as early as 8 h after seeding (**Figure 1a**) and reached a maximum by 72 h (**Figure 1e**). In contrast, cells seeded onto GelMA hydrogels maintained a rounded morphology with little spreading after 8 h of seeding (**Figure 1b**). By 24 h, the average cell area of 416 ± 86 μm^2 on MeTro was 5 times that on GelMA (82 ± 30 μm^2) (**Figure 1j**). A similar trend was seen by the third day where a confluent layer of elongated CMs formed on MeTro but there were only scattered clusters of cells on GelMA (**Figure 1e–f**). Cell spreading areas reached saturation at 1065 ± 99 μm^2 on MeTro by 72 h and 1166 ± 134 μm^2 on GelMA by 192 h. CM attachment was likely facilitated by both the cell-binding motif in tropoelastin and the elasticity of the



Scheme 1. Schematic diagram describing the fabrication of micropatterned gels using a micro-molding process for cardiomyocyte alignment. a) Microchannels with varying channel sizes and spacings were formed on a silicon wafer, to produce a master, which was then covered with a layer of PDMS prepolymer. After curing for 1 h at 80 °C, the PDMS mold was removed and cut into small molds (1 cm x 1 cm); b) a mold was then placed on a glass slide containing 10 μ l MeTro and photoinitiator solution. Exposure to UV light for 35 s crosslinked the hydrogel and generated a micropatterned MeTro gel, the PDMS mold was removed from the gel after soaking in PBS for 5 min; c) the hydrogel containing microchannels was seeded with cardiomyocytes isolated from neonatal rats to align cells within the channels, an unpatterned MeTro gel was used as control.

substratum. Cardiac tissues have been shown to rely on matrix elasticity to preserve cell viability, organization, and tissue function.^[23] MeTro gels are highly elastic with extensibility up to 400%, which is significantly higher than the extensibility of GelMA gels (<100%).^[21] In addition, the tensile modulus of rat CMs of 30 kPa^[26] is closer to the tensile modulus of the MeTro gel used here (\approx 15 kPa) but differs markedly from that of GelMA (\approx 3.8 kPa).^[21]

2.2. Micropatterning of MeTro Hydrogels and CMs Alignment

MeTro gels are amenable to micropatterning. The capacity for exquisite preservation of detailed topography in MeTro hydrogels is surprising, given the abundant literature that presents elastin as an amorphous unstructured mass. Thin films of micropatterned MeTro gels with a typical thickness of 50 μ m were made by UV irradiation of MeTro that was sandwiched between a glass slide and a patterned polydimethylsiloxane (PDMS) mold separated by a 50 μ m spacer (Scheme 1, details are presented in Methods). A UV exposure time of 35 s gave MeTro gels with high pattern fidelity. Patterns were not obtained with shorter exposure times while longer times resulted in the deformation of channels when the mold was peeled off from the gel surface, presumably due to over-crosslinking and adhesion to the PDMS molds. No patterns were generated with 5% (w/v) MeTro prepolymer solution, while micropatterned gels with high pattern fidelities were obtained using 10% (w/v) and

15% (w/v) MeTro at 31% methacrylation. Patterned GelMA gels were cast with 10% (w/v) prepolymer solution and 10 s UV exposure and served as controls in this study.

We made 10% (w/v) MeTro hydrogels with 50 \times 50 μ m and 20 \times 20 μ m regular alternating channel widths and spacings to study the effect of channel size on CM alignment. These molds achieved fine microscale resolution (Figure 2a). In addition to surface micropatterning, MeTro gels of various geometries with well-defined structures were also generated on 3-(trimethoxysilyl) propyl methacrylate (TMSPMA) glass slides by using photomasking (Figure 2b). To the best of our knowledge, this is the first report of high-resolution patterns on the surface of a highly elastic human protein-based gel. Micropatterns have been generated on the surfaces or within 3D structures of various ECM components including fibronectin, collagen, gelatin, and laminin to guide cellular orientation and elongation;^[25–27] however, these materials are neither elastic nor are they comparably mechanically stable. We found that the micropatterns on MeTro surfaces remained stable and without alteration to either their microchannel width size or spacings during 14 days of cell culture. Notably, micropatterned 10% (w/v) GelMA showed pattern deformation after just 7 days

due to their gradual degradation.

We then used micropatterned MeTro and GelMA hydrogels to surface align CMs with the goal of mimicking the anisotropic cell organization of native myocardium. Unpatterned hydrogels served as controls. Cellular alignment and elongation on all substrates were assessed by phalloidin/DAPI staining and revealed that CMs seeded on patterned substrata had oriented with an elongated morphology typical of differentiated CMs along the direction of patterns. However, for cells cultivated on unpatterned surfaces, their actin cytoskeletons were randomly arranged and accompanied by the overlapping of filaments in multiple directions. We saw differences in the shape and orientation of actin filaments as a function of channel size and culture time. Actin filaments were more aligned and elongated on the patterned surfaces with 20 \times 20 μ m channel width and spacing compared to those with larger channel dimensions (50 \times 50 μ m). In addition, culture duration affected the organization of actin cytoskeleton; actin filament alignment was obvious as early as 8 h post seeding and reached its highest level of orientation by day 3 of culture (72 h post seeding). With longer culture times (192 h), the actin filaments overlapped on the surfaces of the gels and their orientations decreased.

Quantitative assessment of cellular alignment as a function of channel size and culture time was performed using DAPI-stained images^[25,28,29] (details are presented in Methods). Cells were considered aligned when the nuclei were oriented within 20° of the microchannel direction. Increasing the channel width from 20 μ m to 50 μ m significantly decreased cellular alignment

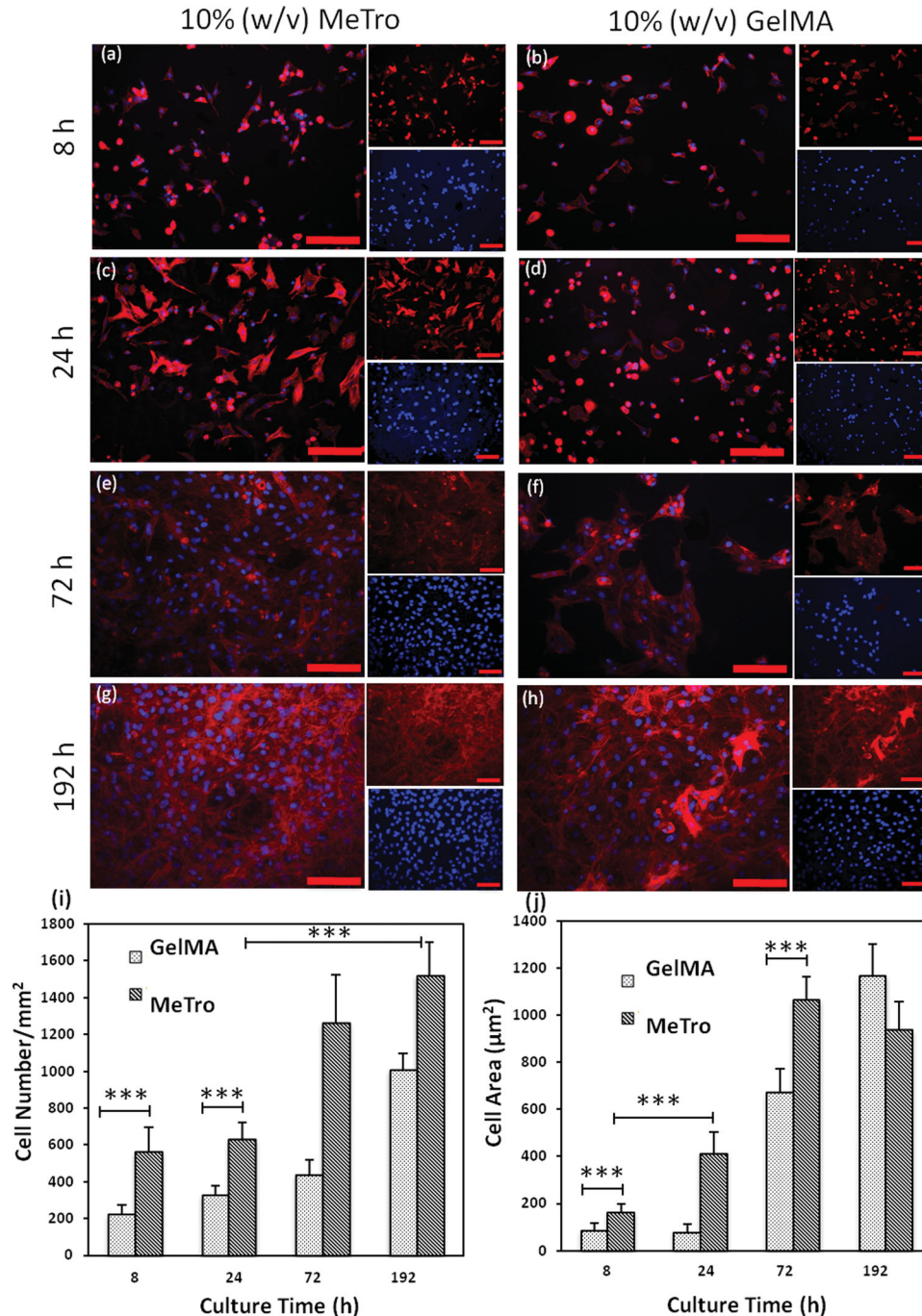


Figure 1. Cardiomyocyte attachment and proliferation on 10% (w/v) MeTro and GelMA hydrogels as a function of time. Rhodamine-labeled phalloidin/DAPI staining for F-actin/cell nuclei of cardiomyocytes seeded on MeTro and GelMA gels after a,b) 8 h, c,d) 24 h, e,f) 72 h, and g,h) 192 h of culture, demonstrating higher cell attachment and spreading on MeTro gels compared to GelMA at different culture times (smaller panels show F-actin (top) and cell nuclei (bottom) stained samples) (scale bar = 100 μm). i) Cell densities, defined as the number of DAPI stained nuclei per given hydrogel area, on MeTro and GelMA gels at various culture times. j) Cell spreading, defined as the area of cell clusters divided by the number of the cells within those cluster, on MeTro and GelMA hydrogels; the reduction in cell area on MeTro compared to GelMA gels after 192 h is a consequence of the higher cell proliferation on MeTro gels. Error bars represent the SD of measurements performed on 5 samples (***) $p < 0.001$.

from $56 \pm 4.8\%$ to $38 \pm 2.9\%$ ($p < 0.001$) (Figure 2c). These findings confirmed the recognized correlation between enhanced CMs alignment and narrow ($\leq 30 \mu\text{m}$) channel widths.^[26,27,30,31]

Our findings agree with those reported for micropatterned laminin coated PDMS surfaces that displayed adhered and

aligned CMs which formed cell-cell junctions preferentially on surfaces with a $20 \mu\text{m}$ periodicity.^[27] Highly oriented sarcomeres were also obtained with micropatterned fibronectin PDMS at the same resolution.^[26] In both of these studies micropatterning techniques were applied to control cellular orientation

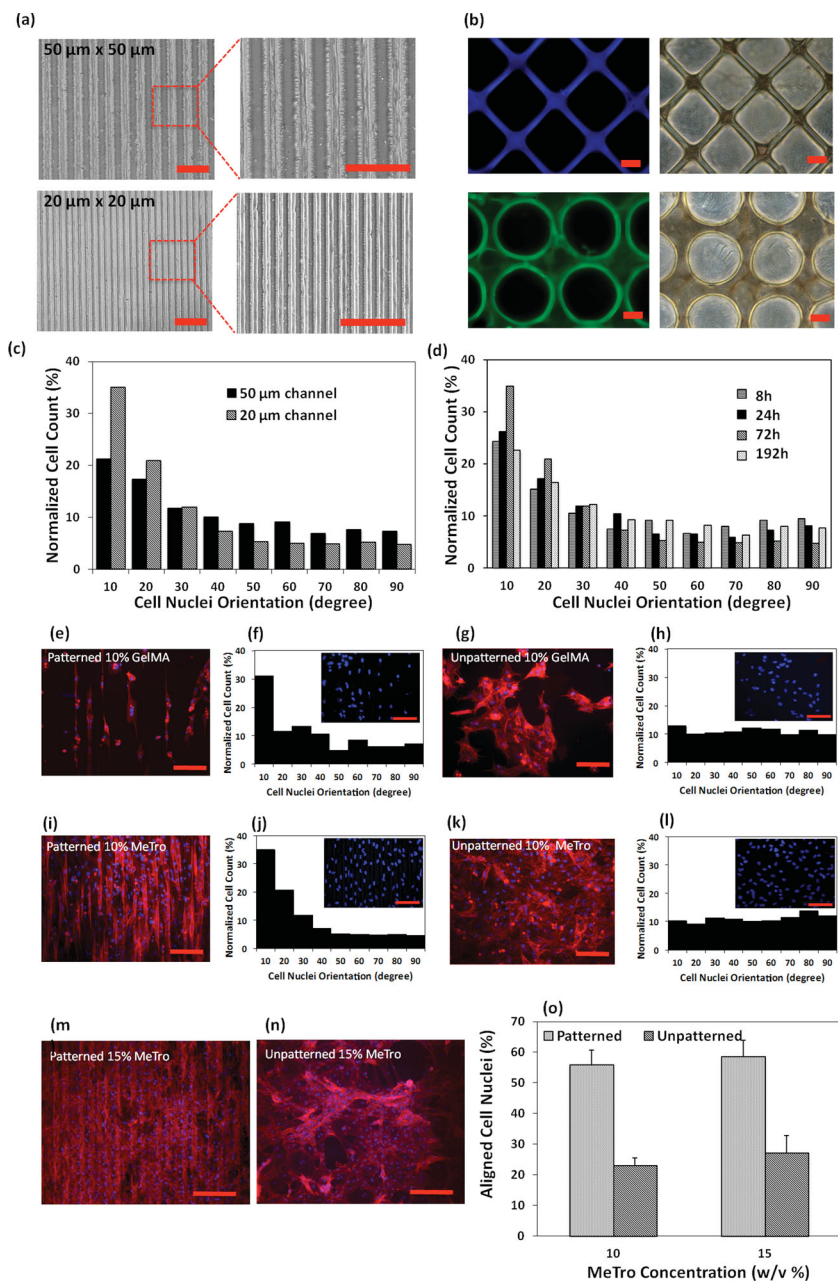


Figure 2. Cardiomyocyte elongation and alignment on the surface of micropatterned gels. Representative images of micropatterned MeTro, a) $20 \times 20 \mu\text{m}$ and $50 \times 50 \mu\text{m}$ channels (scale bar = $200 \mu\text{m}$) produced by micromolding, b) gels of various geometry generated by photomasking (scale bar = $50 \mu\text{m}$). c) Histogram of the relative alignment in 10° increments on day 3 of culture, demonstrating increased cellular alignment with decreasing microchannel width. d) Histogram of the relative alignment obtained at different culture time shows the highest cell alignment after 72 h of culture. Cell alignment on MeTro and GelMA hydrogels 72 h post seeding, representative F-actin/DAPI stained images with corresponding histograms of e,f) patterned GelMA and g,h) unpatterned GelMA; i,j) patterned MeTro; k,l) unpatterned MeTro, demonstrating higher cell alignment in 20° increments on micropatterned MeTro gel compared to patterned GelMA hydrogel (channel size: $20 \times 20 \mu\text{m}$, scale bar = $100 \mu\text{m}$). Effect of MeTro concentration on cardiomyocyte elongation and alignment, representative F-actin/DAPI stained images of cardiomyocytes seeded on m) patterned and n) unpatterned MeTro gels produced by using 15% (w/v) MeTro, o) mean percentage of aligned cell nuclei (within 20° of preferred nuclear orientation), demonstrating cell alignment for both MeTro concentrations.

and resemble the microstructure of the native rat heart, where elongated CMs are tightly positioned between $7 \mu\text{m}$ capillaries that are $\approx 20 \mu\text{m}$ apart.^[32] Here, CMs aligned and elongated along the channels within the $20 \times 20 \mu\text{m}$ micropatterned MeTro to form tissue constructs that mimicked structural features of native heart tissue.

Culture time also affected alignment of the cells on MeTro surfaces. As shown in Figure 2d, alignment was $39 \pm 5\%$ after 8 h of seeding on $20 \times 20 \mu\text{m}$ micropatterned MeTro and increased to $43 \pm 6\%$ and $57 \pm 3\%$ by 24 h and 72 h ($p < 0.001$) then decreased by 192 h following the formation of confluent cells on the gel surface.

On this basis, we used MeTro containing $20 \times 20 \mu\text{m}$ channels and 72 h of culture to compare orientation on patterned and unpatterned MeTro and GelMA gels (Figure 2e–l). Patterned MeTro showed $56 \pm 4.8\%$ aligned cells, which was ≈ 2.5 -fold higher than unpatterned MeTro gels ($23 \pm 2.3\%$ at $p < 0.001$) (Figure 2i–l). Similar results were obtained for patterned and unpatterned GelMA substrates (Figure 2e–h). Micropatterned MeTro exhibited higher cellular orientation than on GelMA gels ($56 \pm 4.8\%$ compared to $42.5 \pm 2.3\%$) ($p < 0.001$). We also observed more attached and elongated cells on 15% (w/v) than on 10% (w/v) micropatterned MeTro surfaces (Figure 2m–o). The substrate made from 15% (w/v) MeTro was covered with a thick layer of CMs that were aligned in the same direction as the microchannels (Figure 2m). Increasing the protein concentration from 10 to 15% (w/v) had no discernible effect on cellular alignment on patterned surfaces; thus CMs can tolerate supramaximal MeTro concentrations.

2.3. Immunohistochemical Analysis

MeTro gels promoted a CM phenotype where cardiac differentiation markers troponin I, sarcomeric α -actinin, and connexin 43 were obvious by day 8. Expression of troponin I was higher on MeTro than GelMA; MeTro facilitated a consistently pervasive, well-developed, contractile apparatus (Figure 3a,b) while CMs displayed smaller aggregates on GelMA (Figure 3c,d). Sarcomeric α -actinin staining on MeTro verified that the cells had developed elongated well-defined, cross-striated sarcomeric structures (Figure 3e,f) that resemble those of native adult rat ventricular myocardium.^[9] In

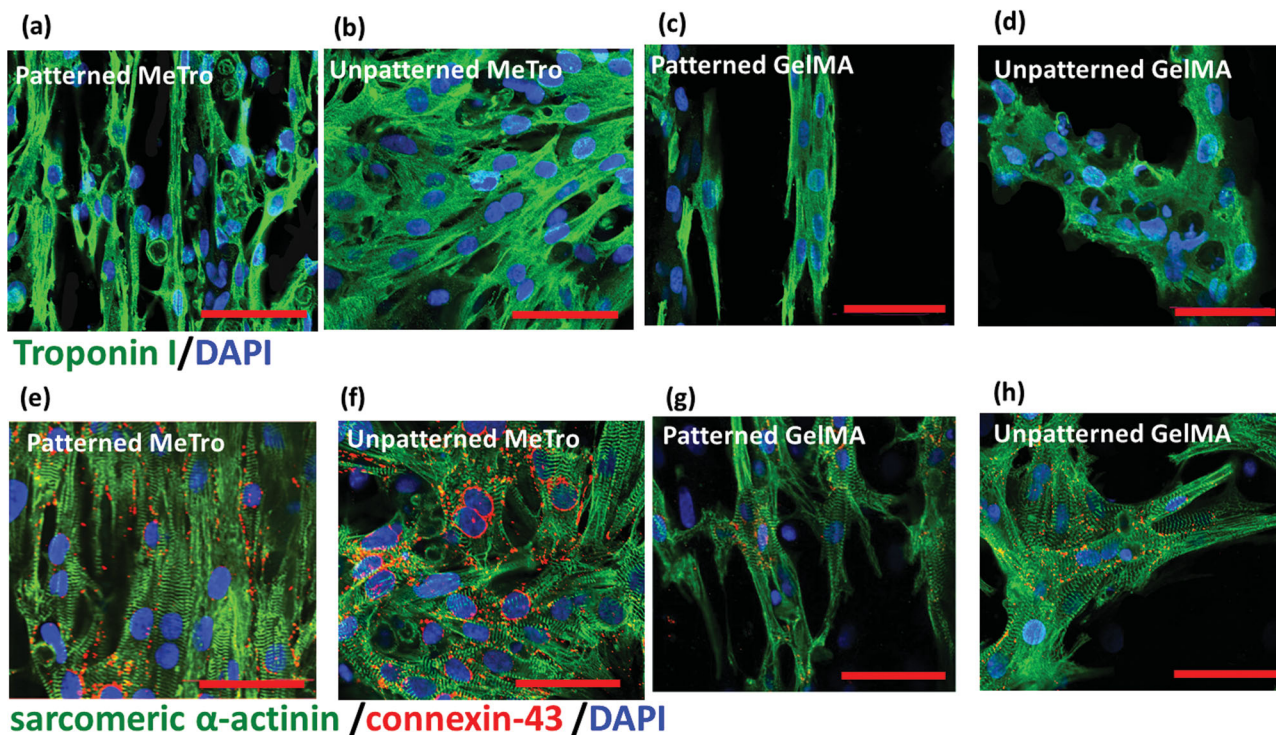


Figure 3. Immunostaining of cardiomyocyte markers. Hydrogels stained for a–d) troponin (green)/nuclei (blue) and e–h) sarcomeric α -actinin (green)/connexin-43 (red)/nuclei (blue) on day 8 of culture, patterned MeTro gels are shown in (a) and (e) and unpatterned MeTro samples in (b) and (f), patterned GelMA in (c) and (g), and unpatterned GelMA in (d) and (h) (scale bar = 50 μ m).

contrast, cross-striations characteristic for mature CMs occasionally appeared for GelMA but only as scattered and poorly organized sarcomeres (Figure 3g,h). In addition, patches of connexin 43 staining were observed in different regions of MeTro gel, demonstrating the presence of well-developed intercalated disk and gap junctions between myocytes. In contrast, on GelMA connexin 43 was sparse and diffuse throughout with occasional cell clusters. We also investigated the effect of cellular patterning on protein expression and found that CM patterning elevated the levels of aligned and elongated cardiac troponin I on surfaces of both gels (Figure 3a,c). In addition, well-aligned registers of sarcomeres developed if the hydrogels were patterned (Figure 3e,g).

In native heart tissue, a large number of gap junctions are present on the lateral surfaces of the CMs for cellular linking and electrical coupling.^[33] The well-developed networks of gap junctions and sarcomeres on MeTro evoke structures of native myocardium. CMs express a higher range of cardiac markers on MeTro gels, which is in agreement with the expectation that ECM proteins are needed to promote CM spreading and maturation due to their ability to provide appropriate cellular cues.^[34,35] We tested the hypothesis that this combination of benefits, in particular the higher level of cell-junctions on cell-seeded MeTro gels, would improve cell-cell coupling accompanied by enhanced overall contractile properties of the engineered tissue constructs, and facilitate synchronous beating.

2.4. Beating Characteristics

The frequency of heartbeats can range from 0.05 to 20 Hz. For example, a whale's heart beats slowly, around 3 to 4 beats min^{-1} (0.05–0.07 Hz) during deep dives, humans around 60–70 beats min^{-1} (1–1.1 Hz), the rat \approx 360 beats min^{-1} (6 Hz), and hummingbirds can achieve 1200 beats min^{-1} (20 Hz) during flight.^[36] CMs seeded on patterned and unpatterned MeTro gels displayed synchronous contractions by as early as 3 days, despite immobilization of hydrogel undersides on glass (Figure 4a,c) (Supporting Information, Videos 1,2). In contrast, CMs on unpatterned GelMA did not beat synchronously (Figure 4b) (Supporting Information, Video 3). On micropatterned GelMA, contractions were stronger and more synchronized than on unpatterned GelMA (Figure 4d) (Supporting Information, Video 4). The beat frequency, quantified between days 4 and 14, varied between 18–60 beats min^{-1} for MeTro (0.3–1 Hz) depending on surface topography of the gel and culture duration (Figure 4e). For unpatterned MeTro surfaces, the beat frequency decreased from 60 ± 9 beats min^{-1} on day 4 to 18 beats min^{-1} on day 10 with no significant changes after that up to day 14 ($p < 0.001$). However, for patterned MeTro gels, the beat frequency was remarkably consistent across the culture time with synchronized beating. Thus surface patterning with MeTro can maintain the contractile activities of cells for at least 2 weeks. However, GelMA patterning had no influence on CM beating over the culture time (Figure 4f). This is likely due to

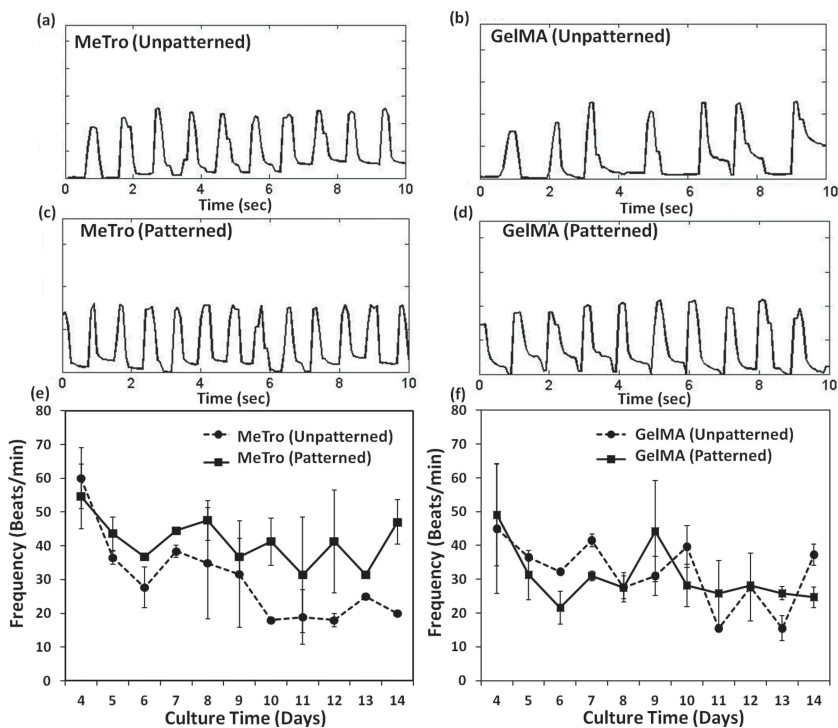


Figure 4. Beating characterization of cardiomyocytes seeded on hydrogels. Beating behavior of cardiomyocyte-seeded a,c) MeTro and b,d) GelMA gels on day 7 of culture, unpatterned samples are shown in (a,b) and patterned ones in (c,d). Spontaneous beating frequency of cardiomyocytes seeded on e) MeTro and f) GelMA gels over 14 days of culture.

the stability of micropatterns on MeTro gels during 14 days of culture, which promoted cell-cell interactions and consequently contractile behavior of the cells. In contrast, pattern deformation was observed after just 7 days on GelMA hydrogels due to their gradual degradation. Therefore, surface patterning on GelMA hydrogels was not as efficient as MeTro substrata in promoting the beating characteristics of CMs. Additionally, the CM beat frequency was generally higher with MeTro than GelMA (e.g., 48 ± 6 beats min^{-1} compared to 27 ± 4 beats min^{-1} on day 8), demonstrating that this elastic hydrogel can support expansion-contraction of cells during beating.

Neonatal rat CMs on hyaluronic acid patterned glass surfaces or Matrigel exhibit spontaneous beating but their contraction frequency decreases with increasing culture time within 7 days of culture.^[37,38] The superior contractile performance of CMs on MeTro material points to its advantages over less elastic biomaterials. It may be that due to its high elasticity and resilience, seeded MeTro substrata could assist contraction in vivo during systole and return to original shape during diastole through this synchronous contraction of CMs.

2.5. Electrical Stimulation

In the native heart, electrical signals are generated by diverse pacing cells causing cell membrane depolarization and activation of the contractile apparatus in CMs^[39] so electrical stimulation would be expected to significantly modulate the CM contractile behavior.^[4,9,38,40–42] Electrical stimulation was applied

to cell-seeded MeTro gels on day 8 in an electrical stimulation chamber (Figure 5a,b). Upon applying electrical stimulation to a physiological medium, a redistribution of charge first occurs, and then, if the stimulus is of sufficient duration, the electrodes will begin to chemically react with the medium to sustain current; this can affect the function of the cardiac tissue construct placed between the electrodes. To minimize this problem, a square-wave pulse with relatively short duration at lower voltage (less than 15 V) was applied according to the previous protocol.^[40] Cells contracted in synchrony in response to electrical field stimulation on patterned and unpatterned gels, and could be paced using 50 ms pulses of electrical stimulation up to 3 Hz. The CMs beating frequency was ≈ 60 beats min^{-1} (1 Hz) before applying electrical stimulation. At each applied frequency, the minimum voltage required to induce synchronized contraction (excitation threshold) was determined by slowly increasing the applied voltage from 0 V until the excitation threshold was reached (Figure 5c, d). Cells pulsed in response to electrical stimuli with more synchronized beating at higher applied voltage. This trend mimics the performance of tissue-engineered myocardial tubes which pulsate at

higher voltage (20 V) but with no response to electrical stimuli at lower applied voltage (e.g., 5 V and 15 V).^[43]

We also investigated the effect of cellular alignment on the CM excitation threshold (Figure 5e). The excitation threshold was lower on micropatterned constructs. For example, at an applied frequency of 2 Hz, the excitation threshold was approximately 1.6-fold higher for unpatterned than on patterned MeTro ($P < 0.05$). Similarly, Engelmayer et al., found that the scaffold microstructure influences the excitation threshold of neural rat heart cells seeded on PGS scaffolds with an excitation threshold of $12 \pm 1\%$ and $17 \pm 2\%$ for accordion-like and rectangular scaffolds, respectively.^[9] We also recorded the synchronous beating signal of the engineered MeTro-based tissue constructs in response to an externally applied electrical field at frequencies ranging from 0.05 Hz to 3 Hz (Figure 5f) and found that increasing the frequency reduced the beating intensity. A combination of surface topography and electrical stimulation influences cardiac cell function. In this study the combined effects of these two factors further improved the functionality of engineered MeTro-based cardiac tissue constructs.

In our study, MeTro provides a model for systematic in vitro studies of CM behavior. As a first step towards the fabrication of 3D cardiac tissue constructs, multi-layered elastic tissue constructs of greater thickness can be generated by assembling tandem layers of cell-seeded micropatterned MeTro gels. However, the thicker scaffolds would probably require vascularization^[44,45] and/or a perfusion system^[38,46] to maintain CM viability. This material lays the foundation for assembling elastic 3D cardiac tissue constructs containing vascular networks

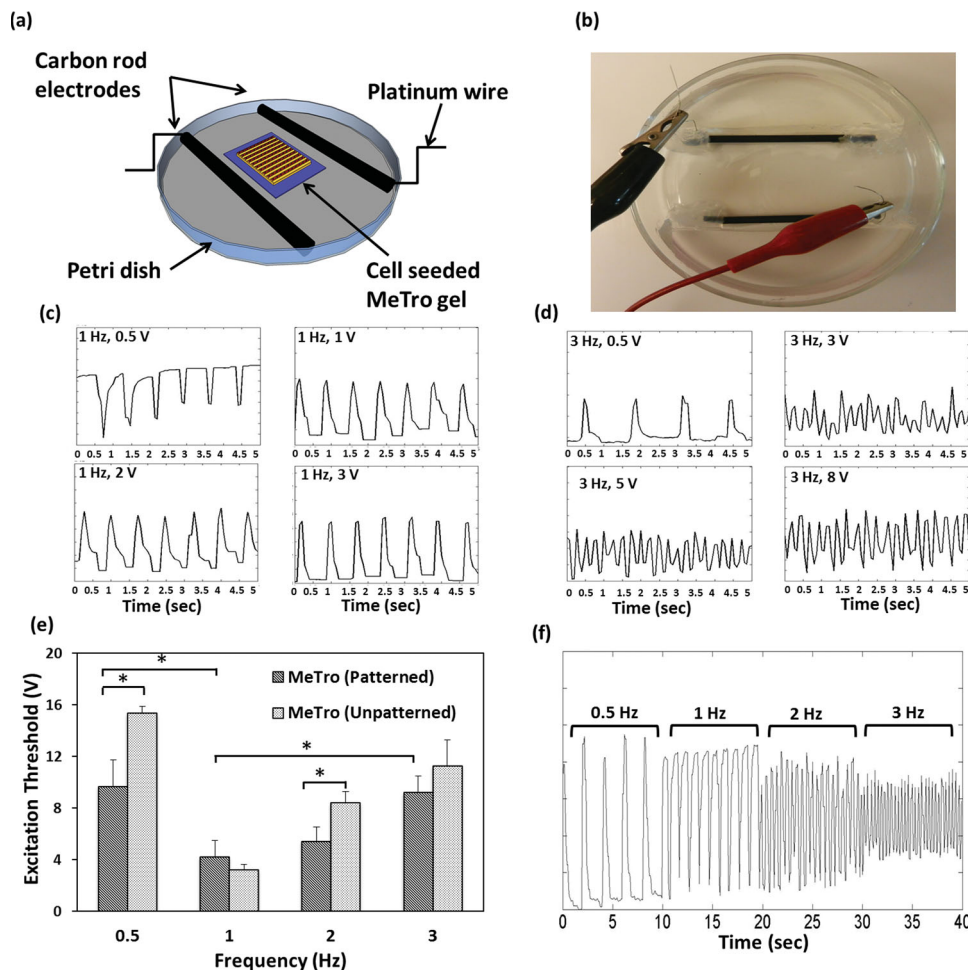


Figure 5. Electrical stimulation of cell-seeded MeTro gels. a,b) Stimulation chamber for applying electrical stimuli to cardiomyocytes cultured on the surfaces of MeTro gels. Analyses of contractile response to electrical stimulation on day 8 of culture, voltage was gradually increased at c) 1 Hz and d) 3 Hz frequencies to induce synchronized beating, the beating became more synchronized by increasing the voltage. e) Excitation threshold of cardiac tissues on both patterned and unpatterned MeTro gels at various frequencies, demonstrating that the excitation threshold was lower in patterned MeTro gels compared to unpatterned ones. f) Recording of synchronous beating signals of cardiomyocytes cultured on patterned MeTro gels in response to applied external electric field at 0.5, 1, 2, and 3 Hz. Error bars represent the SD of measurements performed on 5 samples ($*p < 0.05$).

using MeTro and a spatially distributed co-culture of CM and vascular endothelial cells. Our study also reveals the broader utility of this range of MeTro materials in elastic tissue-mimicking systems.

3. Conclusions

In summary, we have demonstrated the engineering of a novel, highly elastic micropatterned human protein for myocardium regeneration. Our MeTro gels promoted attachment, spreading, and elongation of CMs, which can be due to the cell-interactive amino acid sequence of tropoelastin as well as the similarity of the material's mechanical properties to natural myocardium. In addition, the fabricated MeTro gels were amenable to the microfabrication of a variety of micrometer-sized well-defined geometries. In particular, we generated micropatterns on the surfaces of these hydrogels to align CMs and engineer tissue

constructs mimicking those of the native myocardium. We demonstrated that MeTro gels maintained the phenotype and in vitro contractile properties of CMs. In addition, the functionality of engineered constructs was further improved by applying electrical stimulation to the hydrogels. These microengineered highly elastic constructs establish a versatile and robust foundation for the modeling and regeneration of functional cardiovascular tissues.

4. Experimental Section

MeTro Synthesis: Tropoelastin was methacrylated according to previously outlined procedures.^[21] Briefly, methacrylate anhydride (8% (v/v), MA, Sigma) was added to a tropoelastin solution (10% (w/v)) in phosphate buffered saline (PBS; Invitrogen) to prepare MeTro prepolymer with 31% methacrylation degree. The solution was allowed to react for 12 h at 4 °C and then diluted and dialyzed (Slide-A-Lyzer MINI, 3.5K MWCO) against distilled water at 4 °C for 48 h. The

prepolymer solution was then filtered and lyophilized to yield MeTro macromers. The methacrylation of tropoelastin was confirmed by performing ^1H NMR analysis as previously described.^[21]

Hydrogel Fabrication: MeTro macromers were used to fabricate thin films of photocrosslinked MeTro hydrogels. MeTro gels were prepared by using various concentrations of MeTro solutions (e.g., 5, 10, 15% (w/v)) in PBS containing 2-hydroxy-1-(4-(hydroxyethoxy) phenyl)-2-methyl-1-propanone (0.5% (w/v), Irgacure 2959, CIBA Chemicals). Then, the solution (10 μL) was pipetted between two glass coverslips that were separated by a 150 μm spacer and exposed to 6.9 mW cm^{-2} UV light (360–480 nm) for 35 s. In addition, GelMA hydrogels were prepared by using GelMA (10% (w/v)) with 80% methacrylation degree as described previously^[24] and used as a control.

Surface Patterning: A micromolding technique was used to generate patterns on hydrogel surfaces (Scheme 1). Micropatterned PDMS-based membranes 1 mm thick and with two different channel geometries (channel size \times spacing: 20 \times 20 μm , and 50 \times 50 μm) were formed with negative photoresist Epon SU8. The resultant PDMS molds were then used to pattern the MeTro and GelMA substrates (Supporting Information, Methods). The patterned hydrogels were generated on 3-(trimethoxysilyl)propyl methacrylate (TMSPMA) coated glass slides to covalently bond the hydrogels to the glass slides and avoid hydrogel detachment from the slide during culture. To transfer the PDMS pattern to the surface of MeTro gel, the surface of the PDMS mold was first treated with plasma to create a hydrophilic surface and to facilitate the penetration of prepolymer solution among the channels. Upon crosslinking with UV, the gels were soaked in PBS to facilitate PDMS mold detachment and preserve patterned architecture. The resulting microchannel-containing hydrogels were soaked in culture media at 37 $^{\circ}\text{C}$ for 16 h prior to seeding with neonatal rat CMs. Unpatterned gels were formed by using planar PDMS membranes instead of micropatterned PDMS molds and used as controls.

Surface Seeding (2D Culture): CMs were isolated from 2-day-old neonatal Sprague Dawley rats according to a protocol approved by the Institute's Committee on Animal Care (Supporting Information, Methods). For cell adhesion and proliferation studies on 2D surfaces, MeTro films with 150 μm thickness were prepared on TMSPMA glass slides. The slides containing MeTro were seeded with cells (4×10^5 cells/scaffold) and incubated for 192 h. Media were changed every second day.

The cell-seeded scaffolds were fixed and stained with rhodamine-phalloidin (Alexa-Fluor 594; Invitrogen) and 4',6-diamidino-2-phenylindole (DAPI; Sigma) to visualize F-actin filaments and cell nuclei, respectively (Supporting Information, Methods). Cell proliferation on gel surfaces was assessed by quantifying cell densities, defined as the number of DAPI stained nuclei per given hydrogel area, over the culture time. Rhodamine-phalloidin staining was also used to characterize cell surface spreading over culture time. Cellular alignment on the patterned hydrogels was quantified by measuring the nuclei orientation angles using ImageJ software^[25] (Supporting Information, Methods). Alignment analysis was performed at different culture times for the gels with varying channel geometries. The expression of CM marker proteins on the gels was assessed by immunostaining (Supporting Information, Methods).

Assessment of Contractile Properties of CMs: CM contractile properties on MeTro and GelMA hydrogels were assessed using movies taken with a video camera (Sony XCD-X710) attached to a microscope (Nikon, Eclipse TE 200U, Japan) at 10 \times magnification over 14 days of culture. The microscope was equipped with a temperature controller to maintain the samples at 37 $^{\circ}\text{C}$ during video recording. The video sequences were digitized at a rate of 15 frames per second. To quantify the beat frequency (number of beat min^{-1}), videos taken from 3 selected spots of at least 3 individual samples were analyzed with a custom-written Matlab code for each gel type (MeTro and GelMA). In addition, the effect of patterning on the spontaneous contractions of CMs was determined by using unpatterned MeTro and GelMA gels as controls.

CM Contractile Response Following Applied Electrical Stimulation: The response of CMs to electrical stimulation was assessed by using a modified carbon electrode system to apply a pulsatile electrical signal to

CMs seeded on gels. The electrical stimulation chamber consisted of a petri dish and two carbon rod electrodes.^[40] Two carbon rod electrodes spaced 2 cm apart were placed in a petri dish and fixed in place with silicon adhesive. Two platinum wires were attached on opposite sides of the electrodes by threading through holes drilled into the electrodes and the connections were covered by silicon adhesive (Figure 5a,b). Prior to use, the electrical stimulation chamber was washed with 70% ethanol. To deliver an electrical signal, the engineered construct containing cells was placed between the two parallel carbon rod electrodes. The chamber was then filled with culture media (30 mL) to cover the engineered construct and both electrodes. The electrical pulse generator applied biphasic square waveforms with 50 s pulses delivered at various frequencies including 0.5, 1, 2, 3 Hz. The excitation threshold, minimum voltage required to induce synchronous beating at different frequencies (e.g., 0.5, 1, 2, 3 Hz), was also determined by varying the stimulating voltage from 3 to 15 V at each frequency.

Statistical Analysis: Data were compared using one-way analysis of variance followed by Bonferroni's post-hoc test (GraphPad Prism 5.02) software. Error bars represent the mean \pm standard deviation (SD) of measurements (* $p < 0.05$, ** $p < 0.01$, and *** $p < 0.001$).

Supporting Information

Supporting Information is available from the Wiley Online Library or from the author.

Acknowledgements

N.A. acknowledges the support from the National Health and Medical Research Council. K.T. acknowledges funding from the CRC for Polymers and the BHP-Billiton Fulbright Scholarship. A.K. acknowledges funding from the National Science Foundation CAREER Award (DMR 0847287), the office of Naval Research Young National Investigator Award, the National Institutes of Health (HL092836, DE019024, EB012597, AR057837, DE021468, HL099073, EB008392), and the Presidential Early Career Award for Scientists and Engineers (PECASE). A.S.W. acknowledges funding from the Australian Research Council, Australian Defense Health Foundation and National Health and Medical Research Council. A.S.W. is the Scientific Founder of Elastagen Pty Ltd. The authors declare no conflict of interest in this work.

Received: February 14, 2013

Revised: March 11, 2013

Published online: April 26, 2013

- [1] A. A. Rane, K. L. Christman, *J. Am. Coll. Cardiol.* **2011**, *58*, 2615.
- [2] C. V. C. Bouten, P. Y. W. Dankers, A. Driessen-Mol, S. Pedron, A. M. A. Brizard, F. P. T. Baaijens, *Adv. Drug Delivery Rev.* **2011**, *63*, 221.
- [3] M. Radisic, H. Park, S. Gerecht, C. Cannizzaro, R. Langer, G. Vunjak-Novakovic, *Philos. Trans. R. Soc. Lond. B Biol. Sci.* **2007**, *362*, 1357.
- [4] M. Radisic, H. Park, H. Shing, T. Consi, F. J. Schoen, R. Langer, L. E. Freed, G. Vunjak-Novakovic, *Proc. Natl. Acad. Sci. USA* **2004**, *101*, 18129.
- [5] S. Miyagawa, M. Roth, A. Saito, Y. Sawa, S. Kostin, *Ann. Thorac. Surg.* **2011**, *91*, 320.
- [6] S. Fleischer, T. Dvir, *Curr. Opin. Biotechnol.* DOI: 10.1016/j.bbr.2011.03.031.
- [7] M. Giraud, C. Armbruster, T. Carrel, H. Tevaearai, *Tissue Eng.* **2007**, *13*, 1825.
- [8] T. McDevitt, K. Woodhouse, S. Hauschka, C. Murry, P. Stayton, *J. Biomed. Mater. Res. A* **2003**, *66*, 586

- [9] G. C. Engelmayer, Jr., M. Cheng, C. J. Bettinger, J. T. Borenstein, R. Langer, L. E. Freed, *Nat. Mater.* **2008**, *7*, 1003.
- [10] Y. Wang, Y. M. Kim, R. Langer, *J. Biomed. Mater. Res. A* **2003**, *66A*, 192.
- [11] C. Helary, I. Bataille, A. Abed, C. Illoul, A. Anglo, L. Louedec, D. Letourneur, A. Meddahi-Pelle, M. M. Giraud-Guille, *Biomaterials* **2010**, *31*, 481.
- [12] D. G. Wallace, J. Rosenblatt, *Adv. Drug Delivery Rev.* **2003**, *55*, 1631.
- [13] A. S. Hoffman, *Adv. Drug Delivery Rev.* **2002**, *54*, 3.
- [14] S. F. Badylak, T. W. Gilbert, *Semin. Immunol.* **2008**, *20*, 109.
- [15] M. Papadaki, N. Bursac, R. Langer, J. Merok, G. Vunjak-Novakovic, L. E. Freed, *Am. J. Physiol. Heart Circ. Physiol.* **2001**, *280*, H168.
- [16] N. Bursac, M. Papadaki, R. J. Cohen, F. J. Schoen, S. R. Eisenberg, R. Carrier, G. Vunjak-Novakovic, L. E. Freed, *Am. J. Physiol.* **1999**, *277*, H433.
- [17] P. Camelliti, J. Gallagher, P. Kohl, A. McCulloch, *Nat. Protoc.* **2006**, *1*, 1379.
- [18] N. Annabi, S. M. Mithieux, A. S. Weiss, F. Dehghani, *Biomaterials* **2010**, *31*, 1655.
- [19] S. M. Mithieux, Y. Tu, E. Korkmaz, F. Braet, A. S. Weiss, *Biomaterials* **2009**, *30*, 431.
- [20] S. M. Mithieux, J. E. J. Rasko, A. S. Weiss, *Biomaterials* **2004**, *25*, 4921.
- [21] N. Annabi, S. M. Mithieux, P. Zorlutuna, G. Camci-Unal, A. S. Weiss, A. Khademhosseini, *Biomaterials*, in press.
- [22] D. V. Bax, U. R. Rodgers, M. M. Bilek, A. S. Weiss, *J. Biol. Chem.* **2009**, *284*, 28616.
- [23] C. A. Bashur, L. Venkataraman, A. Ramamurthi, *Tissue Eng.* **2012**, *18*, 203.
- [24] J. W. Nichol, S. T. Koshy, H. Bae, C. M. Hwang, S. Yamanlar, A. Khademhosseini, *Biomaterials* **2010**, *31*, 5536.
- [25] H. Aubin, J. W. Nichol, C. B. Hutson, H. Bae, A. L. Sieminski, D. M. Crokek, P. Akhyari, A. Khademhosseini, *Biomaterials* **2010**, *31*, 6941.
- [26] A. W. Feinberg, A. Feigel, S. S. Shevkopyas, S. Sheehy, G. M. Whitesides, K. K. Parker, *Science* **2007**, *317*, 1366.
- [27] T. C. McDevitt, J. C. Angello, M. L. Whitney, H. Reinecke, S. D. Hauschka, C. E. Murry, P. S. Stayton, *J. Biomed. Mater. Res.* **2002**, *60*, 472.
- [28] J. L. Charest, A. J. Garcia, W. P. King, *Biomaterials* **2007**, *28*, 2202.
- [29] K. S. Brammer, S. Oh, C. J. Cobb, L. M. Bjursten, H. van der Heyde, S. Jin, *Acta Biomater.* **2009**, *5*, 3215.
- [30] N. Bursac, K. K. Parker, S. Iravanian, L. Tung, *Circ. Res.* **2002**, *91*, e45.
- [31] J. Kim, J. Park, K. Na, S. Yang, J. Baek, E. Yoon, S. Choi, S. Lee, K. Chun, S. Park, *J. Biomech.* **2008**, *41*, 2396.
- [32] K. Rakusan, B. Korecky, *Growth* **1982**, *46*, 275.
- [33] K. Baar, R. Birla, M. O. Boluyt, G. H. Borschel, E. M. Arruda, R. G. Dennis, *FASEB J.* **2005**, *19*, 275.
- [34] S. M. LaNasa, S. J. Bryant, *Acta Biomater.* **2009**, *5*, 2929.
- [35] S. Y. Boateng, S. S. Lateef, W. Mosley, T. J. Hartman, L. Hanley, B. Russell, *Am. J. Physiol. Cell Physiol.* **2005**, *288*, C30.
- [36] M. J. Loe, W. D. Edwards, *Cardiovasc. Pathol.* **2004**, *13*, 282.
- [37] A. Khademhosseini, G. Eng, J. Yeh, P. A. Kucharczyk, R. Langer, G. Vunjak-Novakovic, M. Radisic, *Biomed. Microdevices* **2007**, *9*, 149.
- [38] M. Radisic, L. Yang, J. Boublik, R. J. Cohen, R. Langer, L. E. Freed, G. Vunjak-Novakovic, *Am. J. Physiol. Heart Circ. Physiol.* **2004**, *286*, H507.
- [39] N. J. Severs, *Bioessays* **2000**, *22*, 188.
- [40] N. Tandon, C. Cannizzaro, P. H. Chao, R. Maidhof, A. Marsano, H. T. Au, M. Radisic, G. Vunjak-Novakovic, *Nat. Protoc.* **2009**, *4*, 155.
- [41] N. Tandon, A. Marsano, R. Maidhof, K. Numata, C. Montouri-Sorrentino, C. Cannizzaro, J. Voldman, G. Vunjak-Novakovic, *Lab Chip* **2010**, *10*, 692.
- [42] J. M. Karp, Y. Yeo, W. Geng, C. Cannizarro, K. Yan, D. S. Kohane, G. Vunjak-Novakovic, R. S. Langer, M. Radisic, *Biomaterials* **2006**, *27*, 4755.
- [43] H. Kubo, T. Shimizu, M. Yamato, T. Fujimoto, T. Okano, *Biomaterials* **2007**, *28*, 3508.
- [44] S. Sekiya, T. Shimizu, M. Yamato, A. Kikuchi, T. Okano, *Biochem. Biophys. Res. Commun.* **2006**, *341*, 573.
- [45] H. Sekiya, T. Shimizu, K. Hobo, S. Sekiya, J. Yang, M. Yamato, H. Kurosawa, E. Kobayashi, T. Okano, *Circulation* **2008**, *118*, S145.
- [46] T. Dvir, N. Benishti, M. Shachar, S. Cohen, *Tissue Eng.* **2006**, *12*, 2843.